Pharmacophore
(An International Research Journal)
Available online at http://www.pharmacophorejournal.com/
Original Research Paper

PHARMACOPHORE MODELING STUDIES ON 2-ARYLIDENE-4-(SUBSTITUTED ARYL) BUT-3-EN-4-OLIDES

Asif Husain[1]*, Sukhbir Lal Khokhra[2] and Jyoti[2]

[1] Department of Pharmaceutical Chemistry, Faculty of Pharmacy, Jamia Hamdard University, New Delhi -110064, India
[2] Institute of Pharmaceutical Sciences, Kurukshetra University, Kurukshetra, 136119, Haryana, India

ABSTRACT

Three-dimensional pharmacophore hypothesis was built on the basis of a set of known cyclooxygenase inhibitors using PHASE program to understand the essential structural features for cyclooxygenase inhibitors. Four point pharmacophore with one hydrogen bond acceptor (A), one hydrophobic group (H) and two aromatic rings (R) as pharmacophoric features were developed. Amongst them the pharmacophore hypothesis AHRR14 yielded a statistically significant 3D-QSAR model with 0.716 as R^2 value and was considered to be the best pharmacophore hypothesis. The developed pharmacophore model was validated by predicting the activity of test set molecules. The squared predictive correlation coefficient of 0.977 was observed between experimental and predicted activity values of test set molecules.

Keywords: Pharmacophore, QSAR, Coefficient, Furanone, Butenolide.

INTRODUCTION

Pharmacophore modeling is an important approach to quantitatively search common chemical features among a number of structures. A qualified pharmacophore model can be used as a query for searching chemical databases to find out new chemical moieties. Pharmacophore modeling also correlates bio-activities with the spatial arrangement of various chemical features[1]. Pharmacophore mapping[2], a ligand-based drug design approach, and quantitative structure-activity relationship (QSAR) can be utilized in drug discovery in different ways like rationalization of activity trends in compounds under study, prediction of the activity of novel molecules, database search studies in search of new hits and to identify important features for activity[3-6].

Non-steroidal anti-inflammatory drugs (NSAIDs) are widely used in the treatment of different inflammatory conditions. Long term use of NSAIDs has been associated with side effects; especially gastrointestinal[7]. Anti-inflammatory activity of these drugs is mediated by inhibition of cyclooxygenase enzymes (COX-I & COX-II) which causes decreased production of prostanoids[8,9]. The two isoforms of COX have been shown to differ pharmacologically; COX-I is expressed in most of body tissues, COX-II is present with low or undetectable levels in some tissues[9]. Agent which inhibits COX-II, while sparing

COX-1 represents a new therapeutics goal for development of safer non-steroidal anti-inflammatory drugs[10]. Drugs that selectively inhibit COX-II are DUP697, celecoxib, rofecoxib, valdecoxib, etc. The central channel is bigger in COX-II than that of COX-I, this provides 25% larger binding site for inhibitor compound. The larger size and extra nook of COX-II found to be essential features for selective inhibition of this enzyme[11,12].

The butenolide ring, also present in many natural compounds, shows potential biological activities. Butenolides and their pyrrolone analogues have been reported to have potential anti-inflammatory, analgesic, antibacterial, antifungal, antiviral, and antimalarial activities[13-15].

The present study describes the development of a vigorous ligand-based 3D-pharmacophore hypothesis. The pharmacophore hypothesis obtained from the pharmacophoric points is used to derive pharmacophore-based 3D-QSAR model. Such a pharmacophore model provides a rational hypothetical picture of primary chemical features responsible for the activity[3-6,16].

METHODOLOGY

DATASET

The biological data of a series of forty two compounds having anti-inflammatory activity was used for the present study[13]. The anti-inflammatory activity was expressed as % inhibition in rat paw edema volume. The dataset was divided randomly into training set and test set by considering the 70% of the total molecules in the training set and 30 % in the test set. Thirty molecules forming the training set (Table1) were used to generate pharmacophore models and prediction of the activity of test set (12 analogues) molecules was used as a method to validate the proposed model.

Table 1: Experimental anti-inflammatory activity of training set compounds

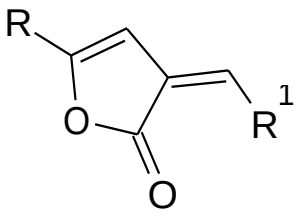

S. No.	R	R^1	% Inhibition	Fitness score
1.	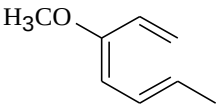	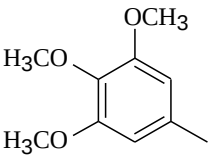	29.03	2.13
2.	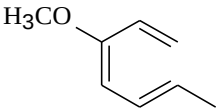	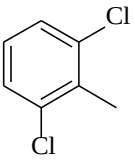	25.80	2.18
3.	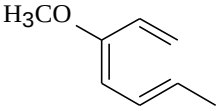	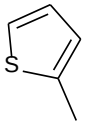	16.12	2.09

4.	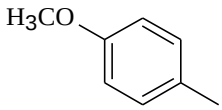	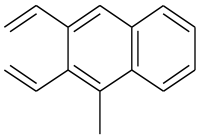	19.35	2.95
5.	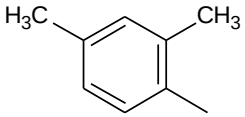	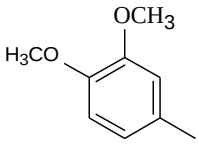	32.25	2.14
6.	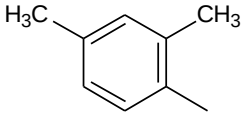	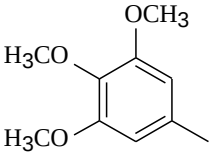	48.38	2.11
7.	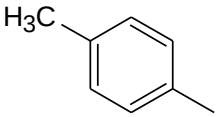	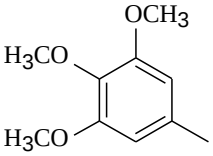	45.16	2.08
8.	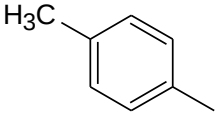	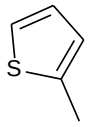	16.12	1.84
9.	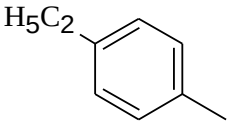	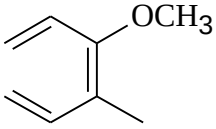	22.58	2.14
10.	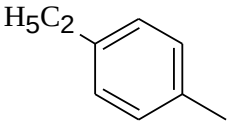	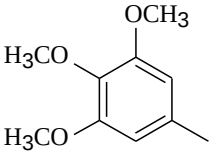	25.8	2.09
11.	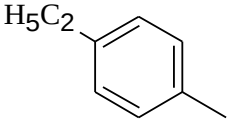	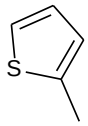	19.35	1.94
12.	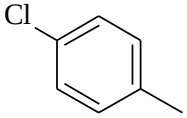	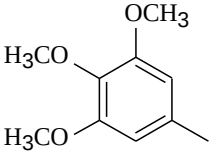	29.03	2.12
13.	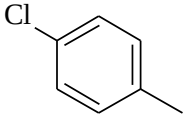	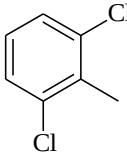	12.9	2.20

14.	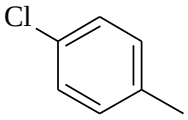	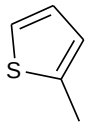	9.67	2.04

.

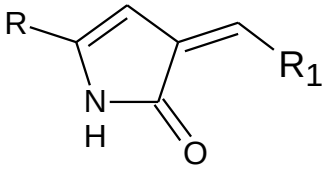

15.	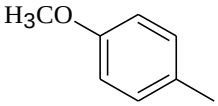	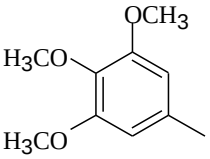	29.03	2.06
16.	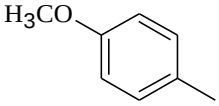	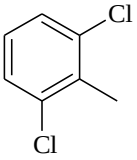	25.80	2.20
17.	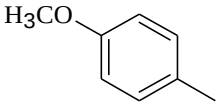	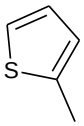	6.45	2
18.	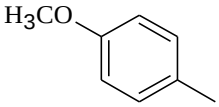	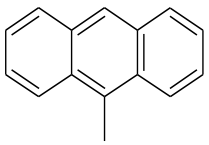	19.35	3
19.	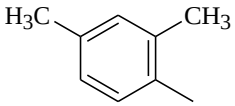	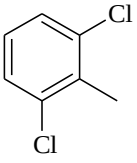	9.67	2.16
20.	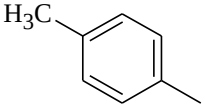	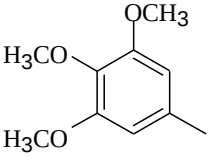	35.48	2.05
21.	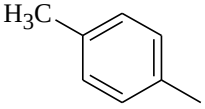	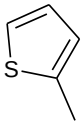	6.45	1.85
22.	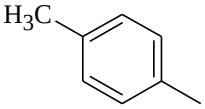	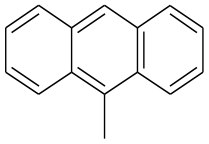	12.90	1.26

23.	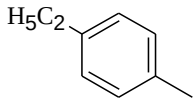	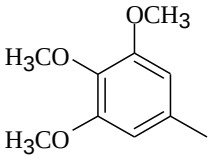	25.80	2.06
24.	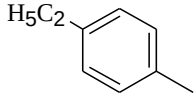	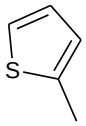	22.58	1.96
25.	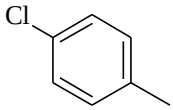	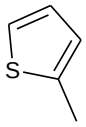	3.22	2.01

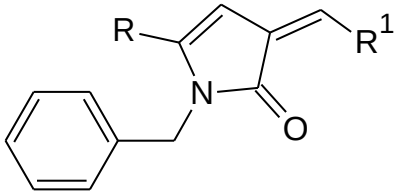

26.	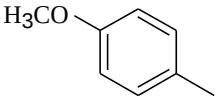	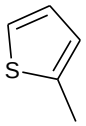	48.38	1.69
27.	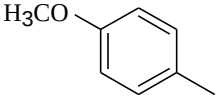	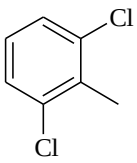	29.03	1.99
28.	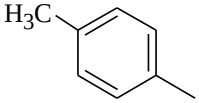	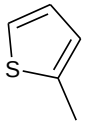	54.83	1.70
29.	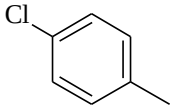	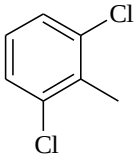	30.42	2.03
30.	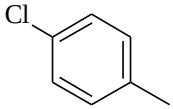	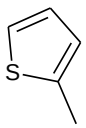	40.03	1.72

Table 1.1: Experimental anti-inflammatory activity of test set compounds

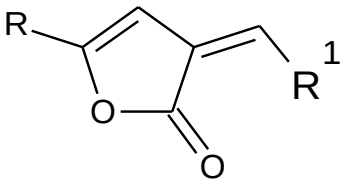

S. No.	R	R^1	% inhibition	Fitness score
1.	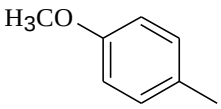	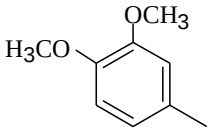	25.8	2.16
2	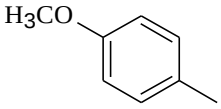	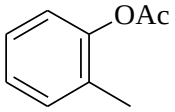	35.48	2.25
3	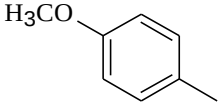	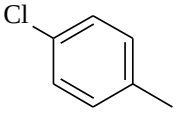	19.35	2.11
4	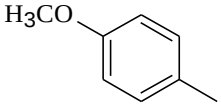	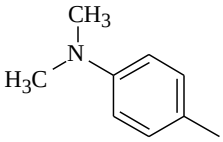	19.35	1.94
5	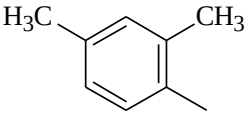	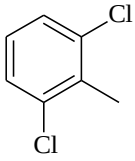	19.35	2.18
6	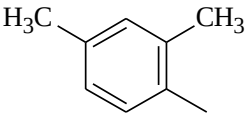	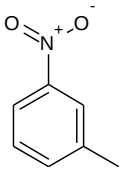	16.12	2.14
7	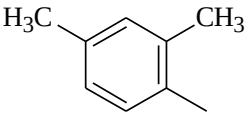	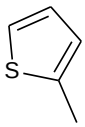	16.12	1.86
8	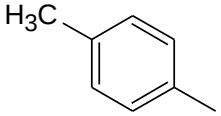	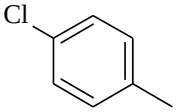	12.90	2.13
9	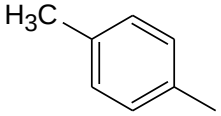	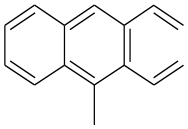	19.35	1.98

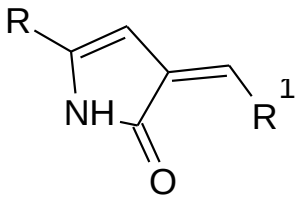

10	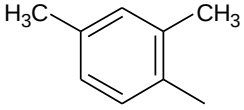	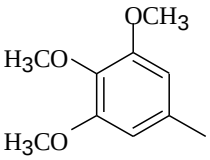	35.48	2.10
11	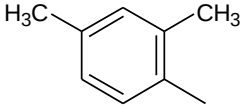	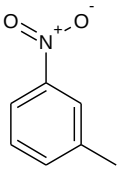	12.90	2.13
12	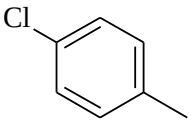	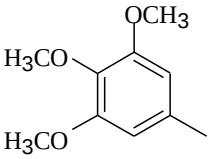	32.25	2.09

PHARMACOPHORE MODELING

Pharmacophore modeling and 3D database searching have now been recognized as essential components of lead discovery and lead optimization. The continuing need for improved pharmacophore based tools has driven the development of „PHASE"[17]. We have used „PHASE": a module of Schrödinger's software program „MAESTRO"[18], to achieve our research objectives.

Preparation of Ligand

Ligand preparation is the primary step for pharmacophore modeling studies. The chemical structures of all the compounds were drawn in maestro and geometrically polished using LigPrep module[19]. LigPrep is a vigorous gathering of tools designed to prepare high quality, all-atom 3D structures for large numbers of drug-like molecules, starting with the 2D or 3D structures in SD or Maestro format. The simplest use of LigPrep produces a single, low-energy, 3D structure with correct chirality"s for each successfully proposed input structure. While performing this step, chirality"s were determined from 3D structure and original states of ionization were retained. Tautomers were generated using Macro Model method discarding current conformers. The conformations were generated by the Monte Carlo (MCMM) method[20,21] as implemented in Macro Model version 9.6 using a maximum of 2,000 steps with a distance-dependent dielectric solvent model and an OPLS-2005 force field[22]. All the conformers were subsequently minimized using truncated Newton conjugate gradient (TNCG) minimization up to 500 iterations. For each molecule, a set of conformers with a maximum energy difference of 30 kcal/mol relative to the global energy minimum conformer was retained. The conformational searches were done for aqueous solution using the generalized born/solvent accessible surface (GB/SA) continuum solvation model.

Creation of Pharmacophoric sites

The second step in developing a pharmacophore model is to use a set of pharmacophore features to create pharmacophore sites (site points) for all the ligands. In the present study, an initial analysis revealed that three chemical feature types i.e., hydrogen-bond acceptor (A), hydrophobic group (H) and aromatic ring

(R) could effectively map all critical chemical features of all molecules in the data set. The minimum and maximum sites for all the features were kept 3 and 5 respectively. These features were selected and used to build a series of hypothesis and find a common pharmacophore option in Phase.

Searching common Pharmacophore

In next step, pharmacophores from all conformations of the ligands in the data set were examined and those pharmacophores that contain identical sets of features with very similar spatial arrangements were grouped together. If a given group is found to contain at least one pharmacophore from each ligand, then this group gives rise to a common pharmacophore. Any single pharmacophore in the group could ultimately become a common pharmacophore hypothesis. Common pharmacophores are identified using a tree-based partitioning technique that group together similar pharmacophores according to their intersite distances i.e. the distances between pairs of sites in the pharmacophore.

Scoring Hypothesis

In scoring hypothesis step, common pharmacophore hypothesis were examined using a scoring function to yield the best alignment of the active ligands using an overall maximum root mean square deviation (RMSD) value of 1.2 Å for distance tolerance. The quality of alignment was measured by survival score[23].

3D-QSAR Model Generation

Phase provides the means to build 3D QSAR models for a set of ligands that are aligned to a selected hypothesis. The Phase 3D QSAR model partitions the space occupied by the ligands into a cubic grid. Any structural component can occupy part of one or more cubes. A cube is occupied by a feature if its centroid is within the radius of the feature. We can set the size of the cubes by changing the value in the Grid spacing text box. The regression is done by constructing a series of models with an increasing number of Partial least square (PLS) factors. In present case, the pharmacophore based model was generated by keeping 1Å grid spacing and 3 as maximum number of PLS factors.

Pharmacophore Model Validation

The validation process is an important part of pharmacophore design. The importance further increased when the model is built for the purpose of predicting activities of compounds in external test series[24]. External validation could be a definite proof for judging predictability of a model. Our priority was to develop QSAR models that were statistically robust both internally as well as externally. The main target of any QSAR modeling is that the developed model should be robust enough to be capable of making accurate and reliable predictions of biological activities of new compounds. In the present case, the developed pharmacophore model was validated by predicting the activity of test set molecules and correlation between the experimental and predicted activities of the test set molecules was done.

RESULTS AND DISCUSSION

In the present study, a series of furanone compounds (butenolides) was considered for molecular modeling studies. The purpose of pharmacophore modeling is to perform *in silico* screening searches in a 3 dimensional database of a virtual or real compound library and to find diverse structures with desired binding activity and selectivity. The studies were aimed at developing a ligand based pharmacophore model relating the anti-inflammatory activity of furanone derivatives.

Thirty molecules forming the training set were used to develop the pharmacophores (Table1). The pharmacophoric features selected for creating sites were hydrogen bond acceptor (A), hydrophobic region (H), and aromatic ring (R). Pharmacophore models containing three, four and five sites i.e. features were

generated. The three featured pharmacophore hypothesis was rejected due to low value of survival score, as they were unable to define the complete binding space of the selected molecules. Five featured pharmacophore hypotheses was also rejected due to non-availability of common pharmacophore.

The results of four featured pharmacophore hypotheses, labelled AHRR14. The hypothesis AHRR14 is the best hypothesis in this study, characterized by highest survival score as shown in Table2. The AHRR14 pharmacophore hypothesis is presented in Figure1. The features represented by this hypothesis are one hydrogen bond acceptor (A), one hydrophobic region (H), and two aromatic rings (R). The angles and distances between different sites of AHRR14 are given in Table 3 and 4, respectively.

Table 2: Different parameters of four featured pharmacophore hypotheses

S. No.	Hypothesis	Survival Score	R^2	F
1.	AHRR14	3.065	0.716	45

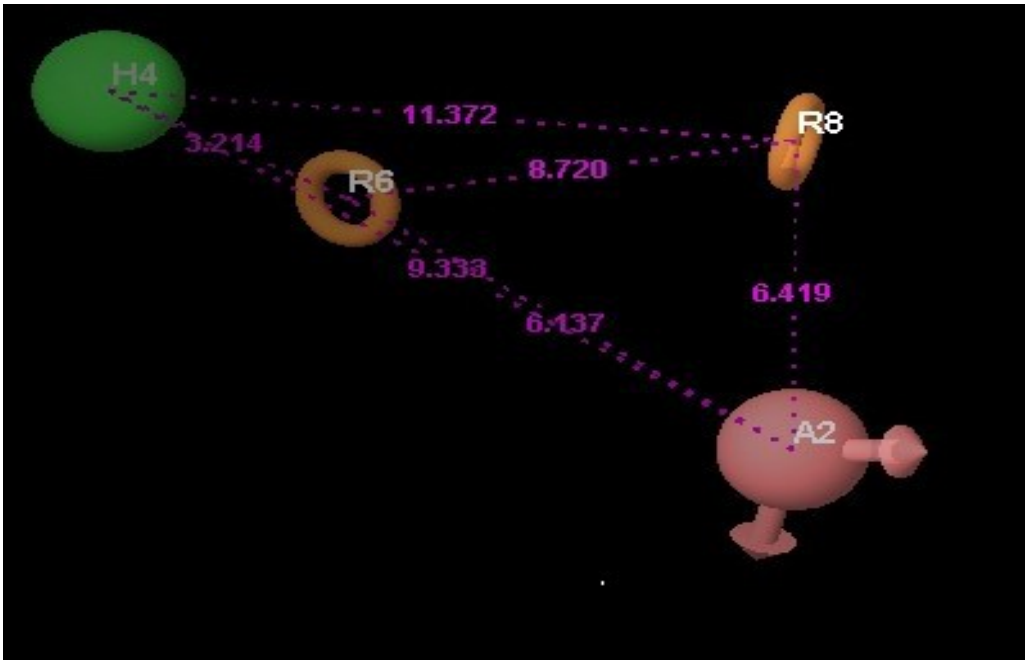

Figure1: PHASE generated pharmacophore model AHRR14 illustrating hydrogen bond acceptor (A2- pink), aromatic ring (R6 and R8 - orange) and hydrophobic ring (H4 - green).

Table 3: Angles between different pharmacophoric sites of model AHRR14

Site 1	Site 2	Site 3	Angle
H4	A2	R6	2.6
H4	A2	R8	90.5

R6	A2	R8	87.9
A2	H4	R6	5
A2	H4	R8	34.4
R6	H4	R8	29.5
A2	R6	H4	172.5
A2	R6	R8	47.4
H4	R6	R8	140
A2	R8	H4	55.1
A2	R8	R6	44.7
H4	R8	R6	10.5

Table 4: Distances between different pharmacophoric sites of model AHRR14

Site 1	Site 2	Distance (A°)
A2	H4	9.333
A2	R6	6.137
A2	R8	6.419
H4	R6	3.214
H4	R8	11.372
R6	R8	8.720

For each ligand, one aligned conformer based on the lowest RMSE of feature atom coordinates from those of the corresponding reference feature was superimposed on hypothesis. Then fitness scores for all ligands were observed on the best scored pharmacophore model. The greater the fitness score, the greater the activity prediction of the compound. The fit function does not only check if the feature is mapped or not, it also contains a distance term, which measures the distance that separates the feature on the molecule from the centroid of the hypothesis feature. Figure 2 shows the AHRR14 aligned with the most active compound 18 (max. fitness score = 3) of the training set.

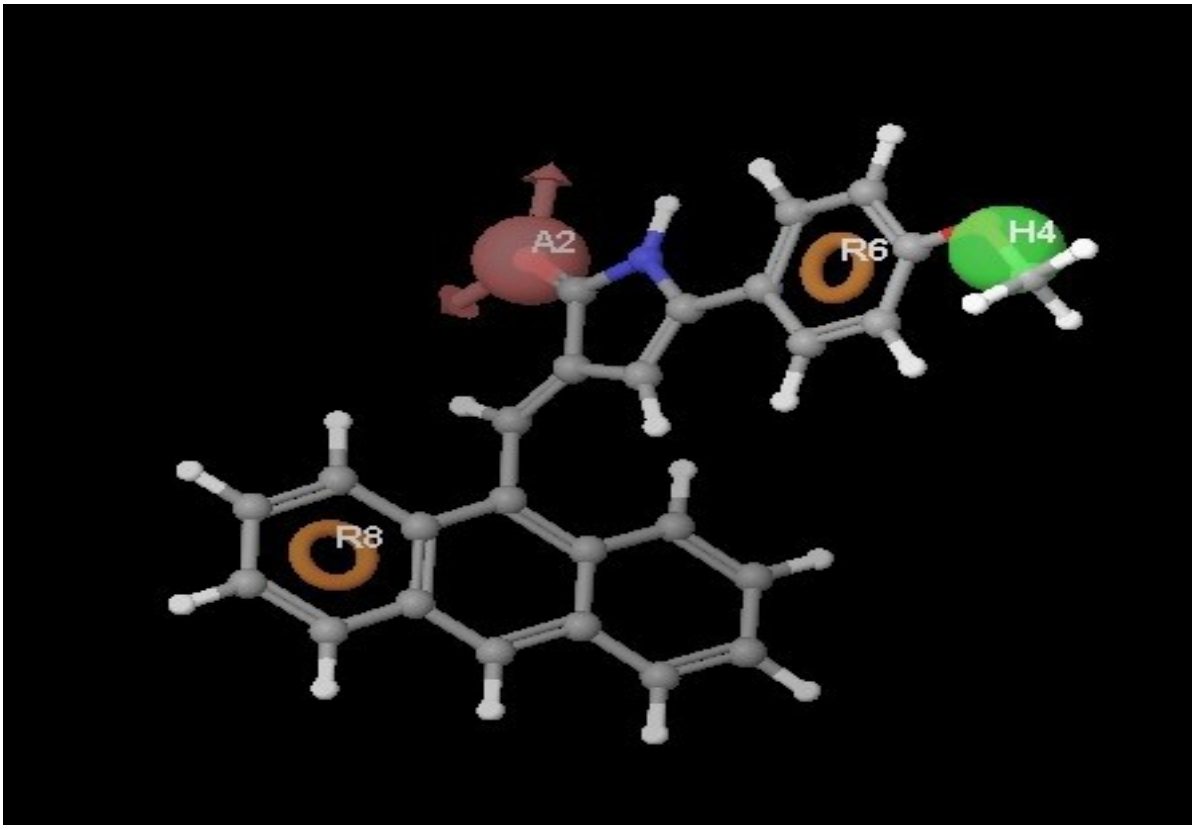

Figure2: Best pharmacophore model AHRR14 aligned with the most active compound 18(maximum fitness score = 3) of the training set. Pharmacophore features are color coded: hydrogen bond acceptor (A2 - pink), aromatic rings (R6; R8 (orange) and hydrophobic ring (H4-green)

Besides this survival score analysis, the validity and predictive character of AHRR14 were further assessed by predicting the activity of test set molecules. A test set having twelve molecules was analyzed. All the test set molecules were built, minimized as well as used in conformational analysis like all training set molecules. Then the activities of test set molecules were predicted using AHRR14 and compared with the actual activity. Actual and predicted activity values of test set molecules are given in Table 6. The predicted anti-inflammatory activity exhibited a correlation of 0.977 using model AHRR14 (Figure4). For a reliable model, the squared predictive correlation coefficient should be >0.60 (25, 26). The results of this study reveal that model AHRR14 can be used for the prediction of anti-inflammatory activity. Good and consistent external predictivity was observed for AHRR14 as compared to the other hypothesis. AHRR14 showed a good R^2 value 0.716 and squared predictive correlation coefficient of 0.977 was observed between experimental and predicted activity values of test set molecules.

Table5: Experimental and predicted activity of training set molecules based on hypothesis AHRR14

Compound	Experimental activity (% inhibition)	Predicted activity (% inhibition)
1	29.03	34.45
2	25.80	20.32

3	16.12	14.32
4	19.35	23.46
5	32.25	30.76
6	48.38	38.27
7	45.16	35.07
8	16.12	19.23
9	22.58	24.37
10	25.80	29.59
11	19.35	16.95
12	29.03	34.10
13	12.90	14.63
14	9.67	12.80
15	29.03	33.71
16	25.80	17.43
17	6.45	12.4
18	19.35	24.48
19	9.67	15.73
20	35.48	33.36
21	6.45	20.06
22	12.90	9.9
23	25.80	27.78
24	22.58	13.47
25	3.22	11.10
26	48.38	54.81
27	29.03	48.46
28	54.83	57.36
29	30.42	35.2
30	40.03	32.2

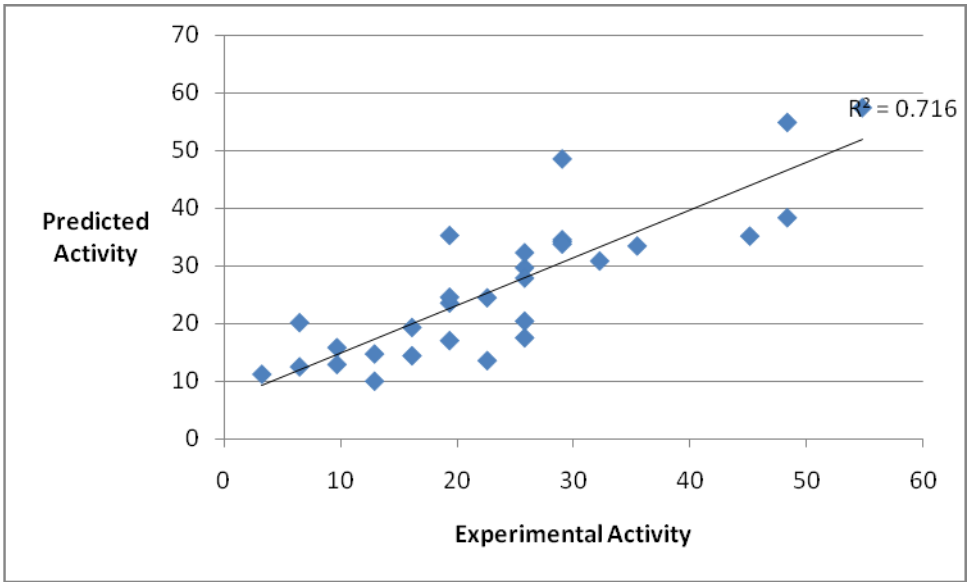

Figure3: Relation between experimental and predicted anti-inflammatory activity values of training set molecules using model AHRR14.

Table 6: Experimental and predicted activity of test set molecules based on hypothesis AHRR14

Compound	Experimental activity (% inhibition)	Predicted activity (% inhibition)
1	25.8	26.17
2	35.48	33.54
3	19.35	20.65
4	19.35	18.09
5	19.35	17.39
6	16.12	16.08
7	16.12	16.23
8	12.90	12.90
9	19.35	18.94
10	35.48	36.21
11	12.90	14.64
12	32.25	32.52

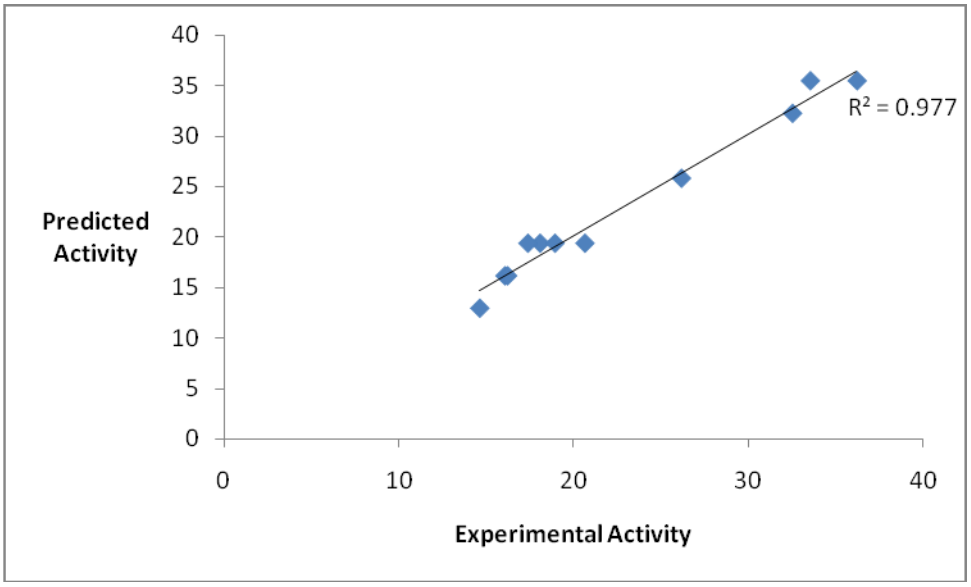

Figure 4: Relation between experimental and predicted anti-inflammatory activity values of test set molecules using model AHRR14

Interpretation of QSAR model

Additional insights into the inhibitory activity can be gained by visualizing the QSAR model in the context of one or more ligands in the series with varying activity. This information can then be used to design new and more active analogues. A pictorial representation of the 3D QSAR models based on compound 18 of the test set using hydrogen bond acceptor, hydrogen bond donor and hydrophobicity features is shown in Figures 5-7. In these representations, the blue cubes indicate favorable regions while red cubes indicate unfavorable regions for activity.

General Structure of Compound 18 of Training Set

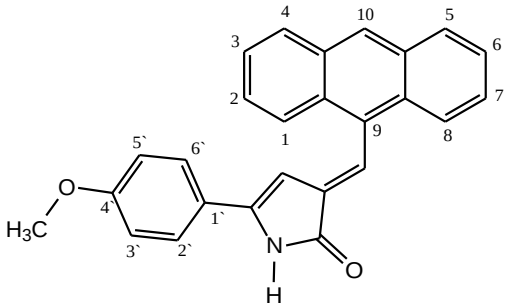

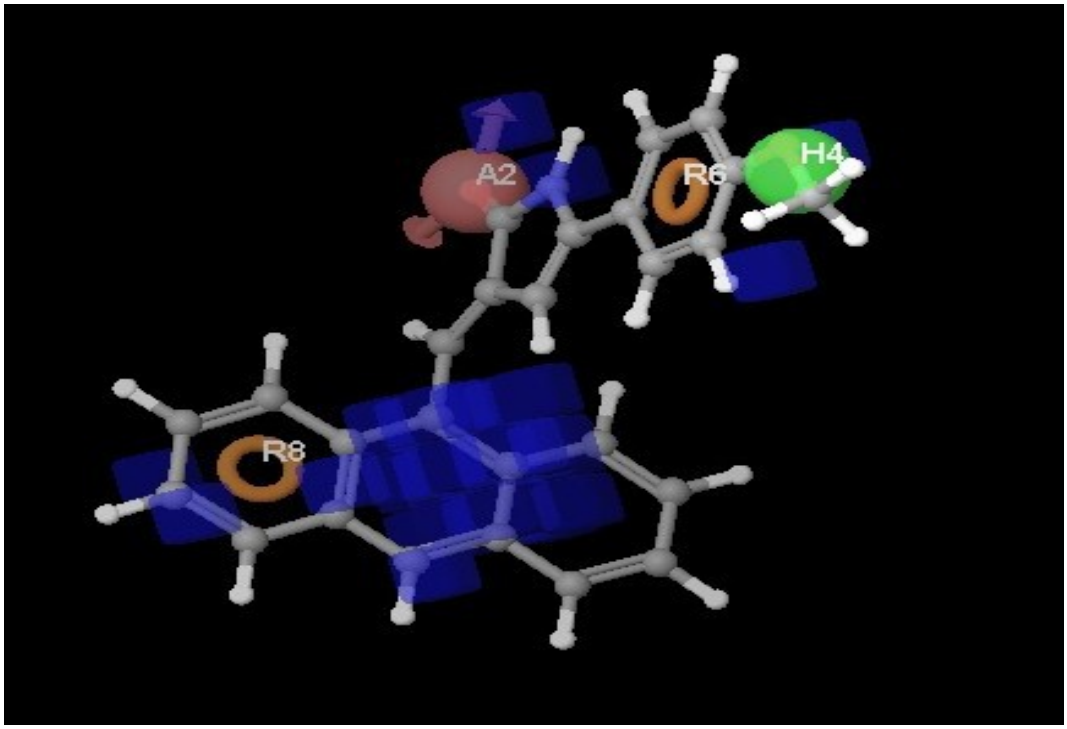

Figure 5: 3D QSAR model based on compound 18 of the training set illustrating hydrogen bond acceptor feature

3D QSAR models based on compound 18 of the training set using hydrogen bond acceptor, hydrophobicity features, and hydrogen bond donor. Figure 5 shows the 3D QSAR model illustrating the hydrogen bond acceptor feature. The blue region in the central ring of anthracene & at carbonyl group of pyrrolone & also adjacent to methoxy group of benzene shows that hydrogen acceptor group at these position causes increase in activity.

The 3D QSAR model based on hydrogen bond donor feature is shown in Figure 6. The red region sows that a hydrogen bond donor group in place of nitrogen of pyrrole ring decreases the activity. Similarly, blue and red regions in Figure 7 indicate the positions where hydrophobic groups will increase and decrease the anti-inflammatory activity respectively. The blue region around nitrogen of pyrrole and at 1` & 3` position of corresponding phenyl ring, at arylidene carbon, and at 3, 4, 5, 6 position of anthracene ring indicates that at these position hydrophobic groups provides good anti-inflammatory activity. Red region 4` & 5` position of benzene ring, at 1 position of anthracene ring results in decreasing activity.

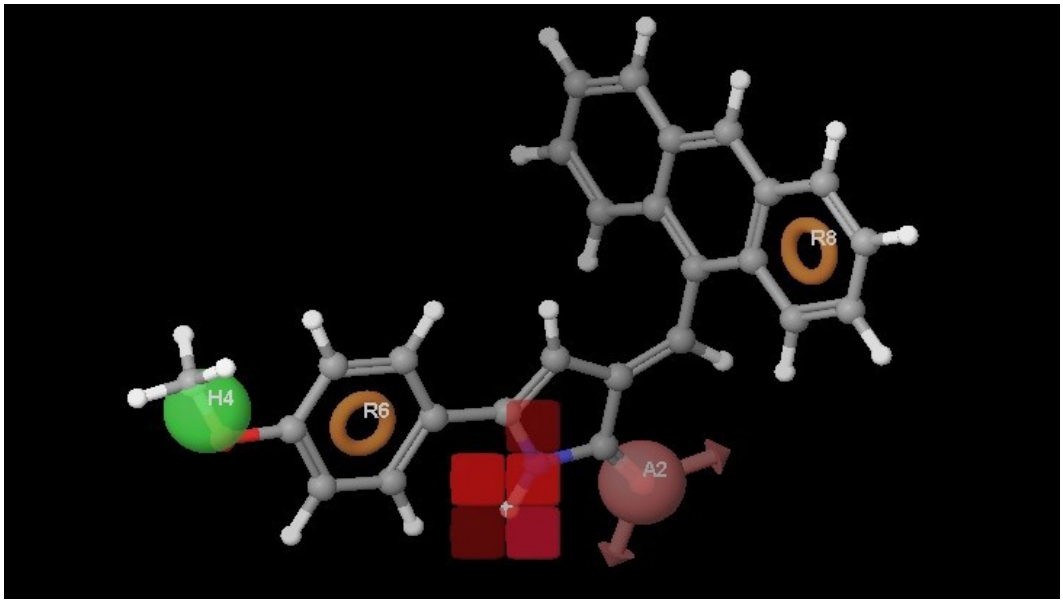

Figure 6: 3D QSAR model based on compound 18 of the training set illustrating hydrogen bond donor feature

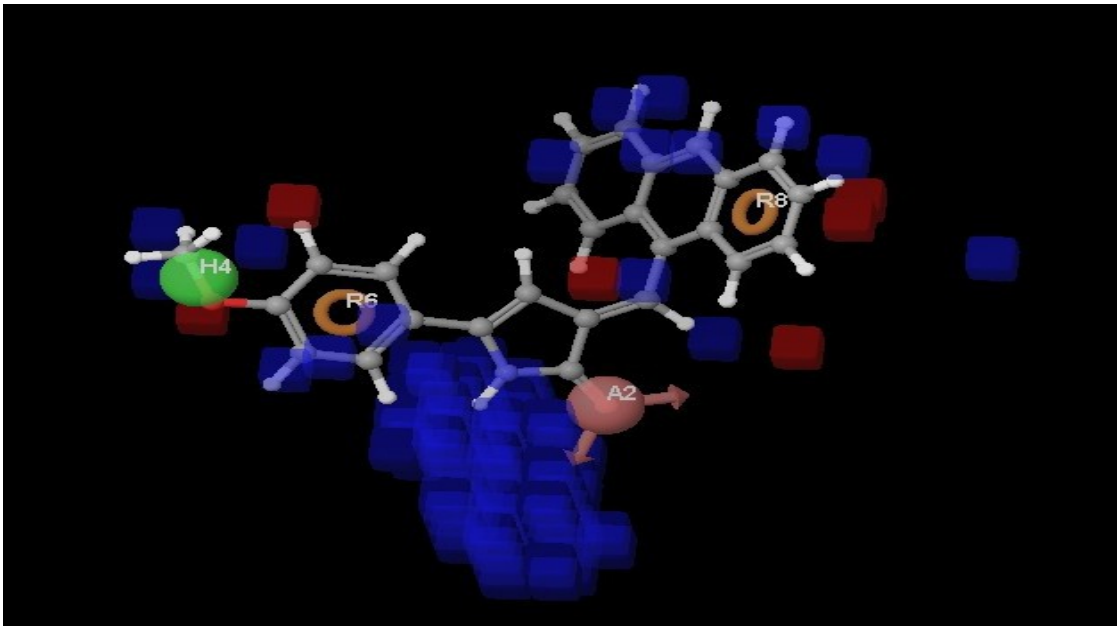

Figure 7: 3D QSAR model based on compound 18 of the training set illustrating hydrophobicity feature

CONCLUSION

The studies show the generation of a pharmacophore model AHRR14 for furanone compounds acting as COX inhibitors. Pharmacophore modeling correlates activities with the spatial arrangement of various chemical features. Hypothesis AHRR14 represents the best pharmacophore model for determining anti-inflammatory activity. AHRR14 consists of one hydrogen bond acceptor, one hydrophobic region and two aromatic ring features. This pharmacophore hypothesis yielded a statistically significant 3D-QSAR model with 0.716 as R^2 value and was considered to be the best pharmacophore hypothesis. The developed pharmacophore model was validated by predicting the activity of test set molecules. The

squared predictive correlation coefficient of 0.977 was observed between experimental and predicted activity values of test set molecules.

This pharmacophore model was able to accurately predict anti-inflammatory activity and the validation results also provide additional confidence in the proposed pharmacophore model.

REFERENCES

1. Sotriffer, CA; Winger, RH; Liedl, KR; Rode, BM and Varga, JM (1996), "Comparative docking studies on ligand binding to the specific antibodies IgE-La2 and IgE-Lb4", ***J. Comp. Aided Mol. Des.***, 10, 305-320.
2. Narkhede, SS and Degani, MS (2007), "Pharmacophore Refinement and 3D-QSAR Studies of Histamine H3 Antagonists", ***QSAR Comb. Sci.***, 26, 744–753.
3. Vepuri, S; Tawari, NR and Degani, MS (2007), "Quantitative Structure-Activity Relationship Study of Some Aspartic Acid Analogues to Correlate and Predict their Sweetness Potency", ***QSAR Comb. Sci.,*** 26, 204-214.
4. Ramar, S; Bag, S; Tawari, NR and Degani, (2007), "3-D-QSAR Analysis of 2-(Oxalylamino) benzoic acid Class of Protein Tyrosine Phosphatase 1B Inhibitors by CoMFA and Cerius 2.GA", ***QSAR Comb. Sci.***, 26, 608-617.
5. Jyoti; Khokhra, SL and Husain, A (2010), "Pharmacophore modeling and 3D QSAR studies on Chalcones as *Trypanosoma cruzi* inhibitors", ***Der Pharma Chemica***, 2(6), 243-255.
6. Khokhra, SL; Husain, A; Jyoti and Jain, S (2011), "Pharmacophore modeling studies on anti-inflammatory butenolides", ***Der Pharmacia Sinica***, 2(4), 241-252.
7. Lanza, FL (1998), "A guideline for the treatment and prevention of NSAID-induced ulcers", ***Am. J. Gastroenterol.***, 93, 2037-2046.
8. Buttgereit, F; Burmester, G and Simon, LS (2001), "Gastrointestinal toxic side effects of non-steroidal anti-inflammatory drugs and cyclooxygenase-2-specific inhibitors", ***Am. J. Med.***, 110, 135-195.
9. Hawkey, CJ (1999), "COX-2 inhibitor", ***Lancet***, 353, 307-314.
10. Khanna, IS; Weier, RM and Collins, PW *et al.* (1997), "1,2-Diarylpyrroles as Potent and Selective Inhibitors of Cyclooxygenase-2", ***J. Med. Chem.***, 40, 1619-1633.
11. Manivannan, F; Prasanna, S and Chaturvedi, SC (2004), "Rationalization of physico-chemical properties of 5,6-diarylthiazolo[3,2-b]-1,2,4-triazoles towards cyclo-oxygenase-2 (COX-2) inhibition: A QSAR approach", ***Ind. J. Biochem. Biophysics***, 41, 179-183.
12. Gierse, JK; MacDonald, JJ; Hauser, SD; Rangwala, SH and Kolbodt, CM (1996), ***J. Biol. Chem.***, 271, 15810.
13. Khan, MSY; Husain, A and Sharma, S (2002), "Studies on butenolides 2-Arylidene-4-(substituted aryl) but-3-en-4-olides: synthesis, reactions and biological activity", ***Ind. J. Chem.***, 41B, 2160-2171.
14. Alam, MM; Husain, A; Hasan SM; Suruchi and Anwer T. (2009), "Synthesis and pharmacological evaluation of 2(3*H*)-furanones and 2(3*H*)-pyrrolones, combining analgesic and antiinflammatory properties with reduced gastrointestinal toxicity and lipid peroxidation", ***Eur.J. Med. Chem.***, 44, 2636-2642.
15. Alam, MM; Sarkar, DP; Alam, O; Husain, A; Marella, A; Akhtar, A; Zaman, MS and Khanna, S (2011), "Search for New Pharmacophore as Antimalarial agent: Synthesis and antimalarial activity of some 2(3*H*)-Furanones bearing quinoline moiety", ***Acta Poloniae Pharmaceutica (Drug Research)***, 68(2), 231-236.
16. Hariprasad, V and Kulkarni, VM (1996), "A Proposed Common Spatial Pharmacophore and the Corresponding Active Conformations of some Peptide Leukotriene Receptor Antagonists", ***J. Comp. Aided Mol. Des.***, 10, 284.

17. PHASE, Version 3.0, Schrodinger, LLC, NY 2008.
18. Maestro, Version 8.5, Schrodinger, LLC, NY 2008.
19. Ligprep, Version 3.0, Schrodinger, LLC, NY 2008.
20. Chang, G; Guida, W and Still, WC (1989), "An Internal Coordinate Monte Carlo Method for Searching Conformational Space", ***J. Am Chem Soc***, 111, 4379.
21. Kolossvary, I and Guida, WC (1996), "Low Mode Search. An Efficient, Automated Computational Method for Conformational Analysis: Application to Cyclic and Acyclic Alkanes and Cyclic Peptides", ***J. Am Chem Soc***, 118, 5011.
22. MacroModel, Version 3.0, Schrödinger, LLC, NY 2008.
23. Tawari, NR; Bag, S and Degani, MS (2008), "Pharmacophore mapping of a series of pyrrolopyrimidines, indolopyrimidines and their congeners as multidrug-resistance-associated protein (MRP1) modulators", ***J. Mol. Model***, 14, 911-921.
24. Boyd, DB (1990), "Successes of computer-assisted molecular design, in: Reviews in computational chemistry", VCH, New York, 355-371.
25. Dureja, H; Kumar, V; Gupta, S and Madan, AK (2007), "Topochemical models for the prediction of lipophilicity of 1,3-disubstituted propan-2-one analogues", ***J. Theo. Comput. Chem.*** 6, 435-448.
26. Wold, S (1991), "Validation of QSAR", ***Quant. Struct. Act. Relat***., 10, 191-193.